Available online at www.sciencedirect.com
ScienceDirect
Marine Chemistry xx (2007) xxx–xxx
MARINE CHEMISTRY
www.elsevier.com/locate/marchem

Modern $CaCO_3$ preservation in equatorial Pacific sediments in the context of late-Pleistocene glacial cycles

R.F. Anderson [a,b,*], M.Q. Fleisher [a], Y. Lao [c], G. Winckler [a]

[a] Lamont-Doherty Earth Observatory of Columbia University, P.O. Box 1000, Palisades, New York 10964, USA
[b] Department of Earth and Environmental Sciences, Columbia University, USA
[c] Department of Laboratory Services, Massachusetts Water Resources Authority, 190 Tafts Avenue, Winthrop, MA 02152, USA

Received 17 August 2006; received in revised form 31 October 2007; accepted 21 November 2007

Abstract

The $CaCO_3$ content of marine sediments in many regions of the ocean has varied systematically with climate throughout the late-Pleistocene glacial cycles. Both biological productivity and carbonate preservation have been proposed to be the master variable regulating this variability. We have evaluated the preserved flux of $CaCO_3$ in cores from the central equatorial Pacific Ocean (~140°W) using the ^{230}Th-normalization technique. Neither barite fluxes nor ^{10}Be/^{230}Th ratios, both geochemical proxies for export production, correlate with $CaCO_3$ fluxes, indicating that productivity is not the principal factor controlling $CaCO_3$ accumulation in these sediments. Preserved fluxes of $CaCO_3$ in central equatorial Pacific sediments correlate in time with the benchmark $CaCO_3$ record from the Cape Basin (South Atlantic Ocean), supporting the view that changes in ocean chemistry (carbonate ion concentration) have controlled the pattern of $CaCO_3$ preservation and accumulation at these sites. Modern $CaCO_3$ preservation in equatorial Pacific sediments has dropped to levels nearly as low as those experienced at any time in the late Pleistocene. Similar changes occurred at the end of each of the late-Pleistocene interglacial periods, from which we infer that ocean carbonate chemistry has already undergone changes that are expected to precede the transition into the next ice age. However, during the late Pleistocene, the time interval between the decrease in $CaCO_3$ preservation and the end of the interglacial has varied substantially from one interglacial to another (from ~2000 to ~15,000 years), so the late-Holocene decrease in $CaCO_3$ preservation cannot be used to predict the end of the Holocene interglacial period.

Keywords: Calcium carbonate dissolution; Paleoproductivity; Holocene duration; Chemical erosion; ^{230}Th-normalization; Equatorial Pacific

1. Introduction

One of the most striking features of the marine geological record is the quasi-regular pattern of variability in the $CaCO_3$ content of sediments found in many regions. This pattern was first described by Arrhenius (1952), who noted that maxima and minima of $CaCO_3$ abundance could be correlated for thousands of kilometers across the equatorial Pacific Ocean. Many subsequent studies have demonstrated that similar patterns occur outside the equatorial Pacific region, for example in the Indian Ocean (e.g., Peterson and Prell, 1985) and in the Subantarctic zone of the Southern Ocean (e.g., Hodell et al., 2001).

* Corresponding author. Lamont-Doherty Earth Observatory of Columbia University, P.O. Box 1000, Palisades, New York 10964, USA. Tel.: +1 845 365 8508; fax: +1 845 365 8155.
E-mail address: boba@ldeo.columbia.edu (R.F. Anderson).

0304-4203/$ - see front matter © 2007 Elsevier B.V. All rights reserved.
doi:10.1016/j.marchem.2007.11.011

For features as widespread as this, one naturally wants to know when and how the variability in the $CaCO_3$ content of sediments was generated, and whether or not the patterns observed in different ocean regions are related to one another. Each of these questions, in turn, leads to more focused inquiry concerning the physical and biogeochemical processes that generated these features.

Consensus was reached long ago concerning "when" these features were formed. Calcium carbonate abundance in sediments of the three regions mentioned above (equatorial Pacific, Indian and Subantarctic Southern Oceans) tends to be at a maximum during late glacial periods and during deglaciation, and at a minimum during times of continental ice sheet growth (e.g., Peterson and Prell, 1985; Farrell and Prell, 1989; Hodell et al., 2001). In contrast to the general agreement concerning the timing of these features, the processes responsible for the variable $CaCO_3$ content of sediments (i.e., "how") have been debated for over half a century (e.g., Arrhenius, 1988; Farrell and Prell, 1989; Archer, 1991; Berger, 1992; Murray et al., 2000). Briefly, the debate centers on the relative importance of biological production of $CaCO_3$ versus $CaCO_3$ preservation as the master variable regulating the $CaCO_3$ content of sediments. Whether control is primarily by production or by preservation, the underlying cause represents a fundamental link between ocean biogeochemistry and climate change. Consequently, the paleoceanographic community has invested a great deal of effort to identify the process(es) responsible.

Evidence in favor of productivity control derives primarily from the apparent co-variation among the accumulation rates in sediments of $CaCO_3$ and of other biogenic phases (e.g., opal, phosphorus, organic matter), which tend to be at a maximum during glacial periods (e.g., Arrhenius, 1952; Pedersen, 1983; Arrhenius, 1988; Lyle et al., 1988; Archer, 1991). Arrhenius (1988) reasoned that one would not expect the accumulation rates of other biogenic phases to be sensitive to changes in $CaCO_3$ preservation, whereas such co-variation would be consistent with control of the $CaCO_3$ content of sediments by biological productivity.

Although the reasoning of Arrhenius is valid, the accumulation rates of equatorial Pacific sediments themselves have become a topic of debate (Marcantonio et al., 1996; Thomas et al., 2000; Marcantonio et al., 2001; Loubere et al., 2004; Lyle et al., 2005; Anderson et al., 2006; Francois et al., 2007; Lyle et al., 2007). Specifically, accumulation rates of biogenic phases in equatorial Pacific sediments that are evaluated by normalizing to ^{230}Th (Francois et al., 2004) do not exhibit the pronounced glacial maxima that are evident in records generated by traditional stratigraphic methods, in which average mass accumulation rates are evaluated between age control points. If the outcome of this debate favors the ^{230}Th-normalization method, then the primary evidence supporting productivity control of $CaCO_3$ variability will be eliminated.

Calcium carbonate preservation is regulated in large part (although not entirely) by changes in the carbonate ion concentration of seawater. Calcite solubility increases with increasing pressure (depth), although there is substantial uncertainty in the actual pressure dependence of calcite solubility (Broecker and Clark, 2007). Nevertheless, all other factors being held constant, at a depth of 4 km an increase in the carbonate ion concentration of 12 μmol/kg would deepen the calcite saturation horizon by about 1 km (Broecker and Clark, 2007). Evidence in favor of preservation (dissolution) control of $CaCO_3$ variability derives primarily from indicators of the degree of dissolution of foraminifera shells ($CaCO_3$), such as etching, pitting, fragmentation, and the relative abundances of dissolution-resistant versus dissolution-prone species (see review by Mekik et al., 2002). Generally, although not always (LaMontagne et al., 1996), minima in $CaCO_3$ abundance are correlated with independent indicators of increased $CaCO_3$ dissolution.

In this study we provide evidence that weighs in on the preservation side of the debate. Our findings support the view that changes in ocean chemistry (carbonate ion concentration) represent the primary factor responsible for $CaCO_3$ variability. Furthermore, by analogy with past interglacial periods, when increased $CaCO_3$ dissolution preceded the build-up of continental ice sheets, the late-Holocene increase in $CaCO_3$ dissolution in equatorial Pacific sediments (e.g., Keir and Berger, 1985; Berelson et al., 1997) suggests that ocean chemistry has already made the change that would precede the earth's transition into the next ice age.

2. Study area, cores, and stratigraphy

Cores used in this study were collected during the US Joint Global Ocean Flux Study (JGOFS) Equatorial Pacific Process Study along a transect normal to the equator at ~140°W (Fig. 1, Table 1). Radiocarbon dates (Table 2) from bulk $CaCO_3$ were used to establish age models for the multicores (MC), and for the upper part of the record from each of the gravity (GC) and piston (PC) cores. Oxygen isotope stratigraphies developed using benthic foraminifera are

Please cite this article as: Anderson, R.F., et al., Modern $CaCO_3$ preservation in equatorial Pacific sediments in the context of late-Pleistocene glacial cycles, Marine Chemistry (2007), doi:10.1016/j.marchem.2007.11.011

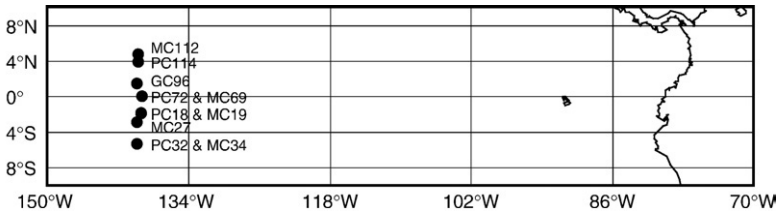

Fig. 1. Locations of cores used in this study. Cores were collected in 1992 during cruise TT013 of the Thomas G. Thompson. MC = Multicore. PC = Piston core. GC = Gravity core. Core locations and water depths are given in Table 1.

available for PC72 at the equator (Murray et al., 1995) and for PC18 at 2°S (Murray et al., 2000). Age models for the other records beyond the range of ^{14}C dating were established by correlating major compositional features (e.g., $CaCO_3$ concentration) with their counterparts in PC18 and PC72 (RFA, unpublished, for GC96, Murray et al., 2000 for PCs). We elected to use GC96 rather than PC83 from 2°N because our initial results from PC83 suggested that some sediment had been lost at the core break between the uppermost two sections of the core.

3. Methods

Preserved fluxes of $CaCO_3$ were derived using the ^{230}Th normalization method (Bacon, 1984; Francois et al., 1990; Francois et al., 2004), which is based on the assumption that the rain rate of particulate ^{230}Th sinking to the sea bed is equivalent to the known rate of ^{230}Th production by ^{234}U decay in the overlying water column. This assumption has found support both in modeling exercises (Henderson et al., 1999; Siddall et al., 2005) and through numerous studies of material collected by deep-sea sediment traps (Scholten et al., 2001; Yu et al., 2001a; Yu et al., 2001b; Scholten et al., 2004).

Table 1
Cores from cruise TT013 used in this study

Core ID [a]	Latitude [b]	Longitude (°W)	Water depth (m)
MC112	5.0783	139.6382	4418
PC114	4.0433	139.8508	4432
GC96	2.0652	140.1493	4417
MC97	2.0500	140.1433	4413
PC72	0.1137	139.4015	4298
MC69	0.1117	139.7233	4307
PC18	−1.8395	139.7137	4354
MC19	−1.8680	139.7157	4376
MC27	−2.8853	139.8317	4513
PC32	−4.9605	139.7436	4236
MC34	−4.9736	139.7373	4256

[a] MC = Multicore, PC = Piston Core, GC = Gravity Core.
[b] Negative values = South.

The principal advantages of this approach are: (1) it allows one to correct for the lateral redistribution of sediments by deep-sea currents (sediment focusing), and (2) the ^{230}Th normalized fluxes are relatively insensitive to errors in the age model of as much as several kyr.

Using this approach, the preserved flux of any sedimentary constituent (Fi) can be estimated as:

$$Fi = Ci \bullet \beta \bullet z / xs^{230}Th_o$$

where Ci is the concentration of the constituent of interest, and $\beta \bullet z$ is the rate of ^{230}Th production in the water column ($\beta = 2.63 \times 10^{-5}$ dpm cm^{-3} kyr^{-1} and z is the depth of the water column in cm). Decay corrections required to obtain the initial unsupported ^{230}Th concentration ($xs^{230}Th_o$) are made using an independent chronology (based on ^{18}O and ^{14}C in this case). An absolute uncertainty in paleo fluxes derived with this method is estimated to be ~30%, based on recent calibration studies (Henderson et al., 1999; Scholten et al., 2001; Yu et al., 2001a; Yu et al., 2001b). However, the point-to-point relative uncertainty in the change in flux through time is much less than this, and in the best case approaches the analytical uncertainty in determining the initial unsupported ^{230}Th concentration.

Uranium and thorium isotopes were measured by isotope-dilution alpha spectrometry (Lao et al., 1993) for the most part, although most samples from TT013-PC72 were analyzed by isotope dilution Inductively-Coupled Plasma Mass Spectrometry (Chase et al., 2003). Concentrations of unsupported ^{230}Th were derived by subtracting from the total (measured) ^{230}Th concentration the amount supported by uranium contained within lithogenic minerals, and any ^{230}Th produced by decay of authigenic U (Lao et al., 1993). These corrections are small in carbonate-rich equatorial Pacific sediments (<3% each throughout the last glacial cycle for all cores;<7% and<11%, respectively, for samples in PC72 at ~300 ka), so the uncertainty introduced by these corrections represents a small component of the overall analytical uncertainty in determining $xs^{230}Th_o$ (2 to 4%, 1 sigma), which results primarily from counting statistics.

The abundance of $CaCO_3$ in all cores was quantified using standard coulometric techniques at the Lamont-Doherty Earth Observatory. In addition, we use $CaCO_3$ concentrations from PC72 reported by Murray et al. (2000) who employed a similar coulometric technique at the University of Rhode Island. There

Please cite this article as: Anderson, R.F., et al., Modern $CaCO_3$ preservation in equatorial Pacific sediments in the context of late-Pleistocene glacial cycles, Marine Chemistry (2007), doi:10.1016/j.marchem.2007.11.011

Table 2
Radiocarbon ages for bulk $CaCO_3$, except where noted, and conversion to calendar age

Lab Code	Description	^{14}C Age	^{14}C Age SD	CALIB 5.0.1 [a])	CALIB 5.0.1	CALIB 5.0.1	Fairbanks0805 [b])	
		(years BP)	(years)	(cal yr+)	(cal yr−)	(cal yr avg)	(cal yr avg)	(cal yr SD)
AA29623	PC72 7–8 cm	4855	65	5656	5482	5569		
AA29624	PC72 12–13 cm	4941	87	5850	5590	5720		
AA20103	PC72 18.5–19.5 cm	6432	62	7422	7314	7368		
AA20104	PC72 27–28 cm	10,643	73	12,808	12,643	12,725.5		
AA29625	PC72 35–36 cm	12,683	94	15,134	14,776	14,955		
AA20105	PC72 47–48 cm	16,246	108	19,503	19,289	19,396		
AA29626	PC72 55–56 cm	20,567	167	24,922	24,350	24,636		
AA20106	PC72 70–71 cm [d]	27,786	113				32,154	117
AA29627	PC72 80–81 cmA	25,672	356				30,263	566
AA29628	PC72 80–81 cmB	26,580	280				31,186	234
AA29629	PC72 95–96 cmA	32,557	514				36,960	543
AA29630	PC72 95–96 cmB	31,775	667				36,227	666
AA29631	PC72 100–101 cmA	35,653	773				40,559	875
AA29632	PC72 100–101 cmB	35,156	695				40,003	942
AA20097	MC69 12–14 cm	6081	61	7147	6805	6976		
AA20098	MC69 22–25 cm	10,095	77	11,954	11,407	11,680.5		
AA20099	PC18 9–10 cm	5209	58	6170	5907	6038.5		
AA20100	PC18 29–30 cm	12,296	89	14,402	14,024	14,213		
AA20101	PC18 49–50 cm	20,232	256	24,545	23,879	24,212		
AA20102	PC18 79–80 cm	28,655	385				32,872	380
AA20108	MC19 1–2 cm	4044	51	4778	4432	4605		
AA20109	MC19 12–14 cm	6625	58	7567	7475	7521		
AA20110	MC19 22–24 cm	11,508	84	13,424	13,269	13,346.5		
AA20093	GC96 24–25 cm	15,625	11	18,924	18,849	18,886.5		
AA20094	GC96 40–41 cm	27,220	31				31,700	76
AA20095	MC97 1–2 cm	5591	66	6435	6304	6369.5		
AA20117	MC97 11–13 cm	9320	69	10,650	10,418	10,534		
AA20096	MC97 27–30 cm	20,524	168	24,855	24,308	24,581.5		
AA20111	PC32 5–6cm TW	6463	118	7474	7267	7370.5		
AA20112	PC32 5–6 cm PC	11,121	120	13,120	12,923	13,021.5		
AA20113	PC32 15–16 cm PC	21,344	214	25,987	25,587	25,787		
AA20114	MC34 1–2 cm	6889	60	7789	7669	7729		
AA20115	MC34 12–14 cm	10,863	76	12,892	12,820	12,856		
AA21116	MC34 20–25 cm	18,317	133	22,068	21,565	21,816.5		
AA20087	MC112 1–2 cm	10,676	90	12,827	12,652	12,739.5		
AA20118	MC112 12–14 cm	25,736	255				255	30,409
AA20088	MC112 25–28 cm	34,965	72				72	39,854
AA20089	PC114 10–11 cm	9273	79	10,569	10,299	10,434		
AA20090	PC114 25–26 cm	12,472	89	14,748	14,265	14,506.5		
AA20091	PC114 40–41 cm	25,290	25				25	29,507
NOSAMS	MC69 0–1 cm [c]	2860	45	3062	2892	2977		
NOSAMS	MC69 10–11 cm [c]	5950	55	6856	6679	6767.5		
NOSAMS	MC69 22–23 cm [c]	10,650	70	12,807	12,658	12,732.5		

All cores are TT013

[a] CALIB = Calendar ages derived using the CALIB radiocarbon calibration program (Stuiver and Reimer, 1993) available at http://radiocarbon.pa.qub.ac.uk/calib using the calibration data set of Reimer et al. (2004).

[b] Fairbanks0805 = Calendar ages derived for samples beyond the range of the CALIB program (21.4 ka) using the algorithm of Fairbanks et al. (2005) available at http://radiocarbon.ldeo.columbia.edu/research/radcarbcal.htm.

[c] Results from picked specimens of *Pulleniatina obliquiloculata* provided by A. Mix and M. Leinen to JGOFS investigators.

[d] Age reversal. This sample was not used in developing the age model for the core.

is no discernable offset in the $CaCO_3$ contents measured in the two labs (see Supplementary online materials), so the two sets of results from PC72 were combined and used without any adjustments or corrections.

4. Results

We use the term "preserved flux" to refer to the fluxes of $CaCO_3$ evaluated by normalizing to ^{230}Th. Neither this method

Please cite this article as: Anderson, R.F., et al., Modern $CaCO_3$ preservation in equatorial Pacific sediments in the context of late-Pleistocene glacial cycles, Marine Chemistry (2007), doi:10.1016/j.marchem.2007.11.011

nor traditional stratigraphic methods used to evaluate sediment accumulation rates provide information about $CaCO_3$ that has been lost to dissolution. Therefore, the method evaluates only that portion of the total flux of $CaCO_3$ raining to the seabed that is "preserved" in the sediments. Preserved fluxes differ from "mass accumulation rates" (g cm^{-2} kyr^{-1}), which are traditionally evaluated as the linear accumulation rate (cm kyr^{-1}) between age control points multiplied by the average *in situ* density (g cm^{-3}) between the control points. Mass accumulation rates encompass both the preserved flux of particulate material raining to the seabed and the net effect of lateral redistribution of particulate material by deep-sea currents. Normalizing to ^{230}Th corrects for lateral sediment redistribution, and gives the preserved fraction of the flux of $CaCO_3$ and other particulate phases raining to the seabed.

Many of the radionuclide data used here to generate $CaCO_3$ fluxes have also been used in previous studies (e.g., Berelson et al., 1997; Marcantonio et al., 2001; Anderson et al., 2006). Those results are archived in the US.JGOFS database (available at http://usjgofs.whoi.edu/jg/dir/jgofs/eqpac/tt013/). Subsequent to the submission of those data to the US JGOFS database in 2002, additional results were obtained for TT013-PC72. Therefore, all of the original data from TT013-PC72 used in this paper are provided in the Supplementary online materials.

4.1. TT013-PC72

Piston core TT013-PC72 contains one of the best-resolved records of the oxygen isotope composition of benthic foraminifera among cores from the central equatorial Pacific Ocean. This is due, in part, to the slightly larger average accumulation rate (1.5 cm/kyr) at this site compared to other cores from this region (Murray et al., 2000). The reliability of the age model for PC72 can be assessed by comparing its oxygen isotope record with the global stack of 57 benthic records compiled by Lisiecki and Raymo (2005). While there may be a slight offset between 150 and 200 ka, the agreement is generally excellent over the past 500 ka (Fig. 2). Good temporal resolution of PC72 is particularly valuable here in that it enables us to precisely locate changes in the $CaCO_3$ content of the sediments, and changes in the preserved flux $CaCO_3$, in the context of glacial–interglacial variability.

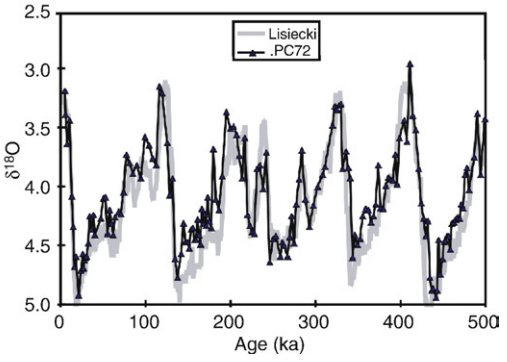

Fig. 2. Oxygen isotopic composition of *Cibicides wuellerstorfi* from TT013-PC72, expressed as $\delta^{18}O$, compared against a stack of 57 benthic oxygen isotope records from sites around the world (Lisiecki and Raymo, 2005). Larger values reflect greater amounts of freshwater stored on the continents as ice. The $\delta^{18}O$ record of PC72 is from Murray et al. (2000). A constant factor of 0.64 has been added to the *C. wuellerstorfi* results, as is conventional for this species of benthic foraminifera.

Concentrations of $CaCO_3$ in PC72 decrease abruptly at, or about, the time of minima in the oxygen isotope record (Fig. 3; note that the oxygen isotope composition, expressed in delta notation, is plotted on a reverse scale). This is consistent with previous studies that have observed decreased $CaCO_3$ abundance during periods of growing ice sheets (increasing $\delta^{18}O$), and it clearly places the onset of declining $CaCO_3$ abundance at close to the time of minimum global ice volume (minimum $\delta^{18}O$).

Changes in the preserved flux of $CaCO_3$ provide a more sensitive indicator than percent $CaCO_3$ of past conditions that influence $CaCO_3$ accumulation in $CaCO_3$-rich sediments. For example, all other factors held constant, a reduction in the $CaCO_3$ content of sediments from 90% to 80% represents a decrease by a factor of two in the $CaCO_3$ accumulation rate, as illustrated in the uppermost part of the record from PC72 (Fig. 4). Over the past 500 kyr, the preserved flux of $CaCO_3$ at the site of PC72 has varied by nearly an order of magnitude (Fig. 4). This range represents a minimum amplitude, because there may have been times in the past when there was net loss of $CaCO_3$ by chemical erosion (i.e., the rate of dissolution exceeded the rain rate of $CaCO_3$ to the sea bed; see Section 5.4). No method of evaluating accumulation rates, including the ^{230}Th-normalization method used here, will give negative values. Therefore, the minimum $CaCO_3$ accumulation rates in Fig. 4 represent upper limits at those times. The true values could have been substantially less, and even negative.

4.2. Meridional transect

Preserved fluxes of $CaCO^3$ extending back into the last glacial period (Fig. 5) were evaluated for cores spanning latitudes from 5°N (MC112) to 5°S (PC32). Two features are immediately evident in these records. First, the pattern of temporal variability in the preserved flux of $CaCO^3$ is consistent from core to core. Later, in the Discussion, we will focus on the record from PC72 with the understanding that it is representative of the larger region, as reflected in the good internal consistency among records in Fig. 5. Second, the spatial pattern of preserved fluxes of $CaCO^3$ between 5°N and 5°S is consistent with the well-established patterns of biological productivity and of the rain of biogenic debris to the sea bed (e.g., Berelson et al., 1997; Murray et al., 2000). Specifically, the greatest fluxes of $CaCO^3$ throughout the last

Please cite this article as: Anderson, R.F., et al., Modern $CaCO_3$ preservation in equatorial Pacific sediments in the context of late-Pleistocene glacial cycles, Marine Chemistry (2007), doi:10.1016/j.marchem.2007.11.011

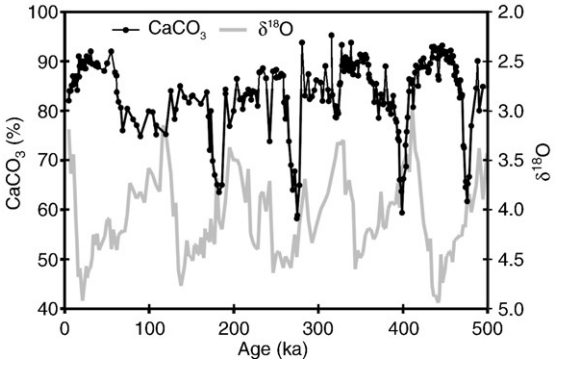

Fig. 3. Calcium carbonate content of TT013-PC72 plotted against age, along with the oxygen isotope record from Fig. 2.

glacial cycle are found at the equator (PC72) and at 2°S (PC18), while the lowest fluxes are found at 5°N (MC112). Intermediate fluxes are recorded at 5°S (PC32), 2°N (GC96) and 4°N (PC114).

5. Discussion

5.1. Reliability of ^{230}Th-normalized fluxes

We have employed the ^{230}Th-normalization technique to evaluate preserved fluxes of $CaCO_3$. Thomas et al. (2000) and Lyle et al. (2005) have questioned the principal assumption inherent in this method, namely that the flux of particulate ^{230}Th to the sediments equals its known rate of production in the water column. They suggest that there may be a substantial net lateral transport by advection and mixing of ^{230}Th from regions of low particle flux (low scavenging intensity) to regions of high particle flux. If true, then this would invalidate the fluxes derived by the technique.

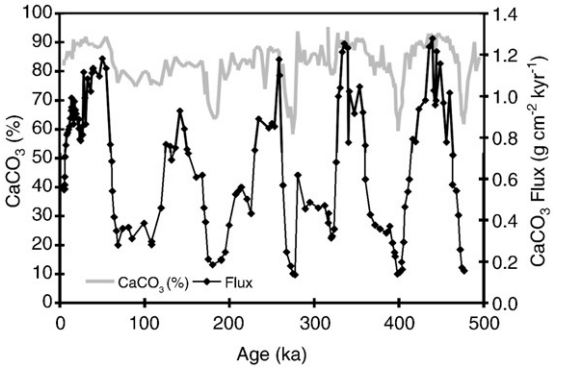

Fig. 4. Concentration (%) and preserved flux (g cm^{-2} ka^{-1}) of $CaCO_3$ in TT013-PC72. Preserved fluxes were evaluated by normalizing to ^{230}Th (see text).

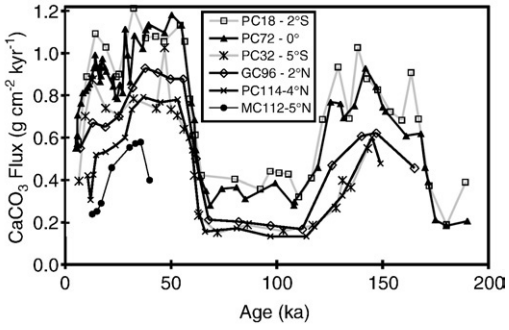

Fig. 5. Preserved fluxes (g cm^{-2} ka^{-1}) of $CaCO_3$ in cores along a section normal to the equator at approximately 140°W (Fig. 1). All cores are from cruise TT013. Preserved fluxes were evaluated by normalizing to ^{230}Th (see text). Core to core differences in the duration of intervals of elevated $CaCO_3$ accumulation reflect a combination of uncertainty in the age models together with the impact of bioturbation and, in some cases, of chemical erosion on the record of $CaCO_3$ accumulation.

Net lateral transport of dissolved ^{230}Th of the magnitude implied by Thomas et al. (2000) and by Lyle et al. (2005) is not supported by observations (see Section 3 above). However, validation in the modern ocean does not prove that the technique is equally valid under different environmental conditions, for example as may have existed during glacial periods. Lacking any absolute standard against which the accuracy of paleo flux reconstructions can be assessed, we use the internal consistency among independent records as a measure for assessing the reliability of the assumptions inherent in the ^{230}Th-normalization technique.

Three points in support of the ^{230}Th-normalization technique can be made based on the internal consistency of results presented here. First, as described above,

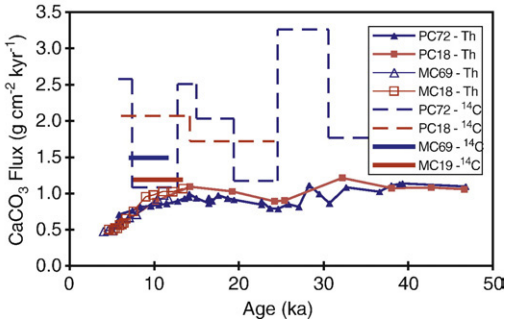

Fig. 6. Calcium carbonate accumulation rates (g cm^{-2} kyr^{-1}) for cores from the equator (PC72 and MC69) and from 2S (PC18 and MC19) evaluated both using the ^{230}Th normalization method and using the traditional stratigraphic method that assumes a constant mass accumulation rate between ^{14}C-dated depths. *In situ* density was estimated using the algorithm of Murray and Leinen (1993) for the ^{14}C-derived accumulation rates. Radiocarbon ages are from Table 2.

Please cite this article as: Anderson, R.F., et al., Modern $CaCO_3$ preservation in equatorial Pacific sediments in the context of late-Pleistocene glacial cycles, Marine Chemistry (2007), doi:10.1016/j.marchem.2007.11.011

similar patterns of temporal variability in the preserved flux of $CaCO_3$ are observed among all of the cores recovered from the transect at 140°W (Fig. 5). Furthermore, the expected spatial pattern, with fluxes at a maximum near the equator (PC72 and PC18) and declining with increasing latitude, is maintained throughout the last glacial cycle.

Second, $CaCO_3$ fluxes evaluated using the ^{230}Th technique are internally consistent among four cores (two piston cores and two multicores) collected at the equator and at 2°S, whereas fluxes derived using ^{14}C dates vary substantially from one core to another (Fig. 6). Cores from the equator and from 2°S offer a good opportunity to test the internal consistency of the two methods because patterns of sediment accumulation at these sites have been similar over recent glacial cycles (Murray et al., 2000). Whether the core-to-core differences observed using ^{14}C age models reflect variable sediment focusing in this region (Marcantonio et al., 1996; Marcantonio et al., 2001) or random errors in the age models (Francois et al., 2007; Loubere and Richaud, 2007) cannot be established with the information available here. However, the greater average fluxes derived using ^{14}C age models may be attributed to sediment focusing in this region.

Third, for PC72 we can compare the preserved flux of $CaCO_3$, derived both using the ^{230}Th-normalization technique (Fig. 4) and using the traditional oxygen isotope stratigraphy (Murray et al., 2000), against an independent record of $CaCO_3$ preservation from another location to see which offers better agreement. The $CaCO_3$ record from ODP Site 1089 in the Cape Basin (40° 56′S, 9° 54′E, 4621 m) provides a benchmark against which the two records from PC72 can be compared. Hodell et al. (2001) noted that the abundance of $CaCO_3$ at Site 1089 follows a pattern typical of the Indian and Pacific Oceans, even though the site is located in the South Atlantic Ocean. Furthermore, by comparing the contrasting patterns of $CaCO_3$ abundance at Site 1089 and at nearby Site 1090 (42° 55′S, 8° 54′E, 3702 m), within the same productivity regime but within a different bottom water mass, they were able to establish that the abundance of $CaCO_3$ at these sites reflects changes in preservation rather than productivity. Site 1089, at a depth of 4621 m, is located below the transition between North Atlantic Deep Water and Southern Source water, within a water mass having chemical properties similar to those of deep Pacific water. Therefore, Hodell et al. (2001) concluded that the down-core pattern of $CaCO_3$ abundance in Site 1089 sediments reflects the changes in deepwater chemistry that have regulated the preservation of $CaCO_3$ in sediments of the Indian and Pacific Oceans.

Preserved fluxes of $CaCO_3$ in PC72 sediments determined using the ^{230}Th-normalization technique agree well with the $CaCO_3$ content of sediments at ODP Site 1089 throughout the past 500 kyr (Fig. 7A.) The pattern of $CaCO_3$ accumulation in PC72 evaluated using oxygen isotope stratigraphy also bears some similarity to the $CaCO_3$ record from Site 1089 (Fig. 7B), but the similarity is substantially less than for the ^{230}Th-normalized $CaCO_3$ fluxes. Therefore, on the basis of the internal consistency among the comparisons presented here, together with evidence presented elsewhere (Francois et al., 2004; Anderson et al., 2006; Francois et al., 2007), we conclude that the ^{230}Th-normalization technique provides a more reliable estimate than traditional stratigraphic methods (e.g., ^{14}C, ^{18}O) of preserved $CaCO_3$ fluxes in central equatorial Pacific sediments.

5.2. Evidence against productivity control

5.2.1. Barite fluxes

Several geochemical proxies for paleoproductivity have been developed (Lochte et al., 2003). Among these,

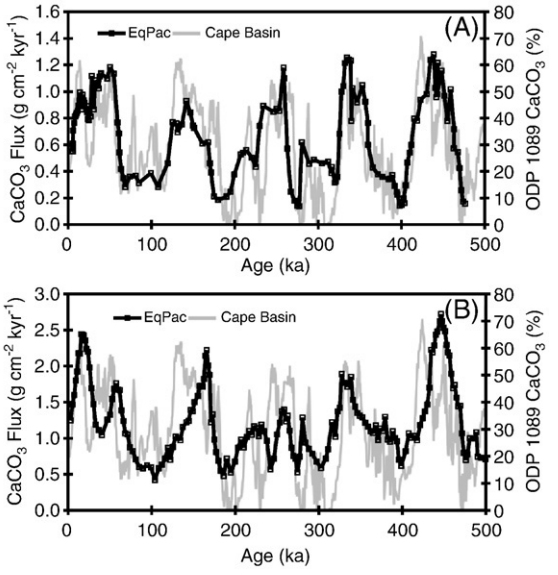

Fig. 7. Accumulation rate of $CaCO_3$ in TT013-PC72 (g cm^{-2} kyr^{-1}) compared against the $CaCO_3$ content (%) of sediments at ODP Site 1089 (Hodell et al., 2001) in the Cape Basin. (A) Accumulation rate (preserved flux) derived using the ^{230}Th-normalization method. (B) Accumulation rate derived using the oxygen isotope stratigraphy for this core (Murray et al., 2000). The age model used for TT013-PC72 is the same in both panels. On average, the $CaCO_3$ flux is larger using the ^{18}O stratigraphy, and this may reflect sediment focusing at the core site (Marcantonio et al., 1996; Marcantonio et al., 2001).

Please cite this article as: Anderson, R.F., et al., Modern $CaCO_3$ preservation in equatorial Pacific sediments in the context of late-Pleistocene glacial cycles, Marine Chemistry (2007), doi:10.1016/j.marchem.2007.11.011

barite, or excess barium, is the one used most widely. Barite fluxes have been linked to export production through sediment trap studies, which have shown that the flux of particulate excess barium (i.e., barium in excess of that contained within aluminosilicate minerals) is well correlated with the flux of organic carbon (Dymond et al., 1992; Francois et al., 1995). Although the origin of the barite is not fully understood, fine-grained barite crystals form within aggregates of decomposing biogenic detritus (e.g., Dehairs et al., 1980; Bishop, 1988; Dehairs et al., 1992). Barite, or excess Ba, offers several advantages over organic carbon in marine sediments as a paleoproductivity proxy. For example, the preservation of barite is generally much greater than that of organic carbon, and less sensitive to environmental variables such as the concentration of oxygen in bottom waters. Furthermore, unlike organic carbon, the barite concentration in marine sediments is not affected by variable contributions from land sources.

The use of barium as a paleoproductivity proxy is not without its own problems, however. For example, preservation of excess barium in marine sediments is greatly reduced under anoxic and suboxic conditions (McManus et al., 1998). Furthermore, barium deposition at continental margins is susceptible to biases associated with the periodic resuspension of barite from continental shelf sediments and lateral redistribution of barite seaward to the continental slope (Fagel et al., 1999). These factors, and others (Fagel et al., 2004), complicate the use of barite as a paleoproductivity proxy in continental margin environments. Nevertheless, in oxic open-ocean sediments, such as those studied here, we expect barite accumulation to provide a reliable proxy for past changes in export production.

Throughout the past 300 kyr, ^{230}Th-normalized barite fluxes in TT013-PC72 exhibit no clear glacial–interglacial pattern of variability, nor any systematic variability that is correlated with preserved fluxes of $CaCO_3$ (Fig. 8). The most prominent feature in the barite record is a minimum flux between 30 and 60 ka, coinciding with the period of greatest sustained $CaCO_3$ flux during the past 300 kyr. Although absolute fluxes evaluated using the ^{230}Th-normalization technique may have uncertainties as large as a few tens of percent, these uncertainties cancel when comparing the fluxes of two constituents in the same core. Therefore, we can conclude with confidence that changes in the preserved flux of $CaCO_3$ as large as a factor of five in PC72 occurred with no detectable correlated change in barite flux, except between 30 and 60 ka when the correlation is negative.

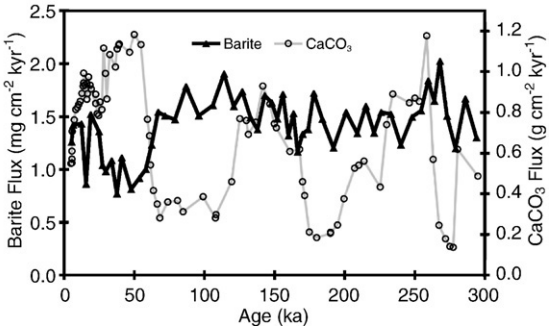

Fig. 8. Preserved fluxes of $CaCO_3$ and of barite in TT013-PC72, both derived using the ^{230}Th-normalization method. Barite concentrations are from Paytan (1995). Barite and thorium samples were offset in depth, typically by no more than 2–3 cm, so ^{230}Th-normalized mass accumulation rates were interpolated onto the depths of the barite samples to estimate barite accumulation rates.

Barite is recognized to be a proxy for the export flux of organic matter, not for $CaCO_3$ production. It is possible that $CaCO_3$ production could vary independently of organic carbon export. However, we are aware of no conceptual model that would account for changes in $CaCO_3$ production as large as the amplitude observed in PC72 in the absence of significant variability in the export flux of organic carbon. Therefore, with the caveat that some mechanism to decouple $CaCO_3$ production from organic carbon export by the large amount required here may yet be discovered, we interpret the barite fluxes to indicate that the variability of $CaCO_3$ accumulation in central equatorial Pacific sediments was not generated by changes in biological productivity.

5.2.2. ^{10}Be/^{230}Th ratios

Ratios of certain naturally-occurring radionuclides (e.g., ^{231}Pa/^{230}Th, ^{10}Be/^{230}Th) have been proposed to serve as proxies for paleoproductivity that are independent of sediment accumulation rate (Kumar et al., 1995). Each of these nuclides is introduced into the ocean in dissolved form (^{231}Pa and ^{230}Th by U decay; ^{10}Be by atmospheric deposition) and each is removed by scavenging onto sinking particles. They differ, however, in terms of their solubility, as expressed by their residence times in the ocean, which vary by more than an order of magnitude (Be>>Pa>>Th). The use of radionuclide ratios as proxies for paleoproductivity derives from the principle that the ratio of a more soluble tracer to a less soluble tracer is expected to increase with increasing particle flux. For example, ^{230}Th is sufficiently insoluble, and its time scale for scavenging from the ocean is so short, that there is little net lateral transport of

Please cite this article as: Anderson, R.F., et al., Modern $CaCO_3$ preservation in equatorial Pacific sediments in the context of late-Pleistocene glacial cycles, Marine Chemistry (2007), doi:10.1016/j.marchem.2007.11.011

dissolved ^{230}Th in the water column between its production by U decay and its removal by scavenging to the sediments. In contrast to ^{230}Th, residence times of ^{231}Pa and ^{10}Be are sufficiently long to permit significant net lateral transport of these species from regions of low particle flux (i.e., low scavenging intensity) to regions of high particle flux between their introduction into the ocean and their removal to sediments. In the open ocean, nearly all of the particle surfaces available for scavenging of radionuclides are of local biological origin. Therefore, radionuclide ratios that increase with increasing particle flux provide a qualitative measure of changes in export production.

Radionuclide ratios are also influenced by the differing affinities among the nuclides for adsorption to various particulate phases (e.g., Chase et al., 2002). For example, it is now recognized that Pa has a strong affinity for adsorption to biogenic opal, and that down-core changes in sedimentary ^{231}Pa/^{230}Th ratios are more directly linked to past changes in diatom productivity than to changes in total export production (Chase et al., 2003). Furthermore, for two of the cores used in this study (TT013-PC18 and PC72), Bradtmiller et al. (2006) have recently shown that ^{231}Pa/^{230}Th ratios are correlated with opal flux over the past 30 kyr, consistent with the findings of Chase et al. (2003). Therefore, we turn our attention to ^{10}Be/^{230}Th ratios as an indicator of past changes in export flux. That strategy was first applied to equatorial Pacific sediments by Marcantonio et al. (2001), and here we revisit their findings.

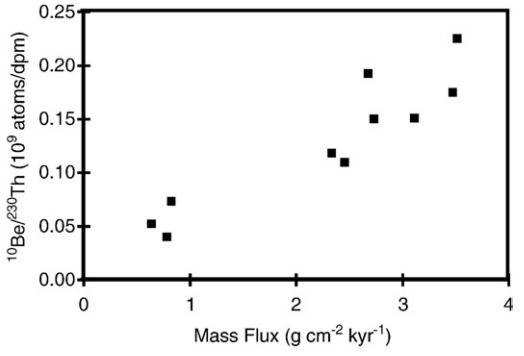

Fig. 9. Flux-weighted annual average ^{10}Be/^{230}Th ratios in time series sediment trap samples plotted against time-weighted mean annual mass flux of particles collected by the sediment traps. Results are presented for traps moored at depths>2000 m and where traps collected particles for a full year. Sediment traps were moored at sites along the US JGOFS transect at 140°W between 9°N and 12°S (Honjo et al., 1995). Figure redrawn from data originally presented in Marcantonio et al. (2001).

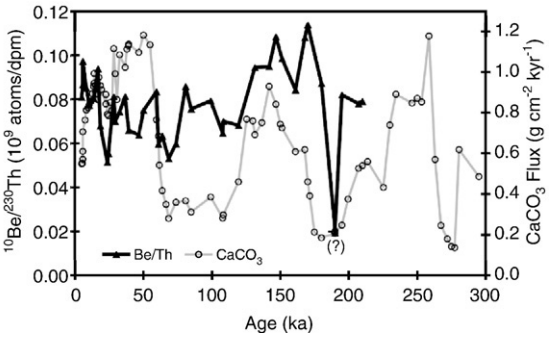

Fig. 10. Initial unsupported ^{10}Be/^{230}Th ratios and preserved flux of $CaCO_3$ plotted against time (years before present) in TT013-PC72. Question mark indicates a low value for which there is no explanation, so it has been kept in the record. ^{10}Be/^{230}Th ratios were originally presented by Marcantonio et al. (2001).

In time-series sediment trap samples collected along the U.S. JGOFS transect at 140°W, the flux-weighted mean annual ^{10}Be/^{230}Th ratio is well correlated with the time-weighted mean annual flux of particulate material (Fig. 9). This is consistent with the principles described above concerning the differing solubilities of the two radionuclides. While ^{10}Be/^{230}Th ratios may also be influenced by particle composition (Chase et al., 2002), the nearly linear relationship observed in these results (Fig. 9) indicates that particle flux is the principal factor regulating the ^{10}Be/^{230}Th ratios.

If the pronounced variability of preserved $CaCO_3$ flux in equatorial Pacific sediments were generated by changes in biological productivity, then we would expect to find these down-core features correlated with ^{10}Be/^{230}Th ratios. However, we find no such correlation between ^{10}Be/^{230}Th ratios and $CaCO_3$ flux (Fig. 10). Except for a single low value that cannot be explained, ^{10}Be/^{230}Th ratios exhibit little variability through time, reminiscent of the ^{230}Th-normalized barite fluxes, and no discernable relationship to the preserved $CaCO_3$ fluxes.

Absolute values of ^{10}Be/^{230}Th ratios in PC72 sediments are lower than in sediment trap samples from the same location (among the highest values in Fig. 9), reflecting the different sources and scavenging behavior of the two nuclides. Whereas ^{230}Th is produced and scavenged uniformly throughout the entire water column, ^{10}Be is introduced and scavenged primarily from surface waters, and particulate ^{10}Be experiences some regeneration at depth. Consequently, particulate ^{10}Be/^{230}Th ratios are observed to decrease with increasing water depth where sediment trap samples have been collected at multiple depths (Chase et al., 2002). The lower ^{10}Be/^{230}Th ratios found in PC72 sediments,

Please cite this article as: Anderson, R.F., et al., Modern $CaCO_3$ preservation in equatorial Pacific sediments in the context of late-Pleistocene glacial cycles, Marine Chemistry (2007), doi:10.1016/j.marchem.2007.11.011

compared to sediment trap samples from shallower depths at the same site, simply reflect a continuation of that trend.

Each of the paleoproductivity proxies describe here (barite flux and $^{10}Be/^{230}Th$ ratios) is sensitive to multiple factors (e.g., biological productivity, preservation, particle composition). Viewed in isolation, the record from either proxy would have to be interpreted with caution. However, the two proxies provide internally consistent results in that neither exhibits the correlation with preserved flux of $CaCO_3$ that would be expected if variability of the $CaCO_3$ flux were regulated by biological productivity. The fact that the two proxies are based on independent principles lends confidence to our conclusion that export production in the central equatorial Pacific Ocean has remained relatively constant throughout recent glacial cycles (see also Winckler et al., 2005), and that variability in the preserved flux of $CaCO_3$ reflects changes in preservation rather than production.

5.3. Indirect evidence for preservation control

Similar patterns of $CaCO_3$ accumulation have been found at various sites around the world, and this similarity supports the view that these patterns are regulated primarily by variable $CaCO_3$ preservation associated with changes in the carbonate ion concentration in deep water. Hodell et al. (2001) noted that temporal variability in the $CaCO_3$ content of sediments at ODP Site 1089 in the deep Cape Basin bears a strong resemblance to records of $CaCO_3$ dissolution indices at two locations in the Indian Ocean (Peterson and Prell, 1985; Bassinot et al., 1994) as well as in the equatorial Pacific Ocean (Le and Shackleton, 1992). Hodell et al. (2001) reasoned that the strong similarity among these records more likely reflects preservation than productivity because deepwater chemistry (carbonate ion concentration) is expected to be similar at these sites whereas one would not expect to find similar patterns of biological productivity among these diverse regions. This reasoning was further supported by the contrasting records of $CaCO_3$ accumulation at ODP Sites 1089 and 1090, which could be explained by changes in preservation, but not by changes in productivity (Hodell et al., 2001).

Internal consistency between ^{230}Th-normalized fluxes of $CaCO_3$ in TT013-PC72 and the $CaCO_3$ content of sediments at ODP Site 1089 (Fig. 7A) reinforces the view expressed by Hodell et al. (2001). Following a strategy analogous to theirs, we ruled out biological productivity as the principal factor regulating temporal variability in the preserved flux of $CaCO_3$ in PC72. Internal consistency among sites as different as the equatorial Pacific and the Subantarctic Southern Oceans strengthens the view that global changes in deep water chemistry, rather than biological productivity, created the observed patterns of $CaCO_3$ accumulation.

5.4. Modern $CaCO_3$ preservation in the context of past variability

5.4.1. Chemical erosion

The abundance and accumulation rate of $CaCO_3$ in equatorial Pacific sediments have declined throughout the late Holocene (Keir and Berger, 1985; Yang et al., 1990; Berelson et al., 1997). Preservation indices indicate that this trend is associated with increased $CaCO_3$ dissolution (e.g., Mekik et al., 2002). At sites near the equator along the transect at 140°W (Fig. 1; 2°S, Eq., 2°N) dissolution of $CaCO_3$ in surface sediments, evaluated using benthic flux chambers, is approximately equal to the rain rate of $CaCO_3$ to the seabed, evaluated using sediment traps (Berelson et al., 1997). At increasing distances from the equator, especially along the northern fringe of the carbonate oozes that occur under the equatorial upwelling system, the rate of $CaCO_3$ dissolution may now exceed the rain rate of particulate $CaCO_3$; that is, chemical erosion may be occurring.

Chemical erosion implies that the sediment–water interface is moving downward with time as the loss of $CaCO_3$ by dissolution exceeds the combined rate of delivery of $CaCO_3$ and of phases that are preserved in the sediments. As the sediment–water interface moves downward, bioturbation exhumes older sediments, adding to the bioturbated mixed layer some $CaCO_3$ bearing an old radiocarbon age. Old ^{14}C ages of surface sediments provided the first clue that chemical erosion is taking place in equatorial Pacific sediments (Broecker et al., 1991; Keir and Michel, 1993). Subsequently, modeling of ^{230}Th profiles in surface sediments provided additional evidence for chemical erosion (Berelson et al., 1997; Stephens and Kadko, 1997).

The effects of chemical erosion are evident in TT013-MC112 from 5°N, where the ^{14}C age of bulk $CaCO_3$ at a depth of 1–2 cm, converted to calendar age, is 12740 years (Fig. 11). Bioturbation extends to a depth of ~10 cm at this site, estimated as the interval over which the $CaCO_3$ content exhibits a nearly linear gradient. This gradient reflects the combined effects of bioturbation together with loss of $CaCO_3$ at the sediment–water interface and the addition of $CaCO_3$-rich sediments at the base of the mixed layer. A ^{14}C date

Please cite this article as: Anderson, R.F., et al., Modern $CaCO_3$ preservation in equatorial Pacific sediments in the context of late-Pleistocene glacial cycles, Marine Chemistry (2007), doi:10.1016/j.marchem.2007.11.011

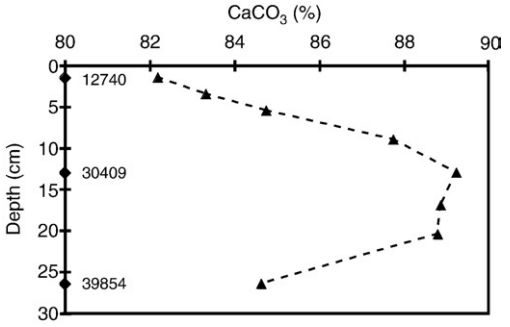

Fig. 11. Concentration profile of $CaCO_3$ in TT013-MC112 (5°N). Values corresponding to points inside the Depth axis represent radiocarbon ages converted to calendar years (Table 2).

from $CaCO_3$-rich sediment just below the mixed layer gives an age (30,409 cal yr BP) coinciding with the period of maximum $CaCO_3$ accumulation in PC72 (Fig. 4). Apparently, chemical erosion has completely obliterated sediments deposited during Marine Isotope Stage (MIS) 2 (13–27 ka), and is now exhuming older sediments deposited during MIS 3.

It is not clear if chemical erosion is occurring at other sites along the US JGOFS transect. Radiocarbon ages (Table 2) from the 1–2 cm depth interval are fairly old in MC34 (5°S) and in MC97 (2°N), but these cores lack the dramatic increase in ^{14}C age below the mixed layer seen in MC112 (5°N). If chemical erosion is occurring at 5°S and 2°N, as suggested by modeling ^{230}Th profiles (Berelson et al., 1997; Stephens and Kadko, 1997), then it is less severe than at 5°N. In any case, $CaCO_3$ dissolution has intensified during the late Holocene, and the $CaCO_3$ profiles in equatorial Pacific sediments are not presently at steady state.

5.4.2. Changes in deep water chemistry

Assuming that the production of $CaCO_3$ has remained relatively constant through time (Section 5.2), fluxes of $CaCO_3$ collected by sediment traps deployed along the transect at 140°W (Honjo et al., 1995) can be compared against the maximum preserved $CaCO_3$ fluxes recorded in the sediments to assess the maximum state of $CaCO_3$ preservation during the last glacial cycle. Sediment traps were deployed for one year during the US JGOFS process study, so they did not record the interannual variability of biogenic fluxes that is known to occur in this region (Berelson et al., 1997). Despite this added uncertainty, the differences are large enough to reveal two important points.

First, the spatial pattern of maximum preserved $CaCO_3$ fluxes, which occurred during MIS 3 at all sites (Fig. 12, triangles), is remarkably similar to the pattern of $CaCO_3$ fluxes collected by sediment traps (Fig. 12, diamonds). In both cases, fluxes are greatest near the equator and decrease slightly to the north and to the south. To a first approximation, the difference between sediment trap flux and maximum preserved flux is uniform across the study area. We interpret this difference to reflect a relatively constant dissolution rate of $CaCO_3$ throughout the region superimposed on a spatially varying rate of supply.

Second, for each site, the maximum preserved $CaCO_3$ flux is less than half the corresponding $CaCO_3$ rain rate collected by deep sediment traps (Fig. 12), indicating that most of the $CaCO_3$ rain was dissolved, even during times of maximum preservation. Furthermore, this comparison may represent an upper limit for the maximum fraction of $CaCO_3$ preserved in the sediments, because fluxes of particulate biogenic material during the US JGOFS study in 1992 may have been slightly below the long-term average for this region due

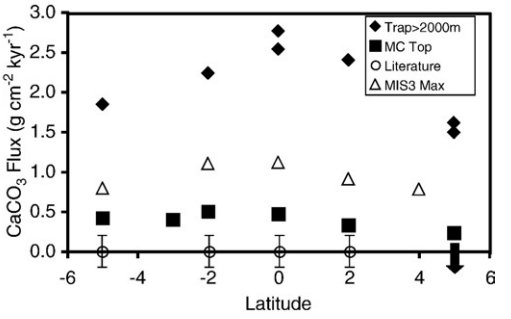

Fig. 12. $CaCO_3$ fluxes versus latitude along the US JGOFS transect at 140°W. Diamonds represent annual average fluxes collected by sediment traps deployed at depths greater than 2000 m (Honjo et al., 1995). Values are shown only for traps that collected particles for a full year. Where two values are shown at a latitude, the results represent traps deployed at different depths. $CaCO_3$ fluxes collected by sediment traps were evaluated by normalizing to ^{230}Th (^{230}Th results for sediment trap samples are archived at http://usjgofs.whoi.edu/jg/dir/jgofs/eqpac/) to allow comparison against fluxes in sediments evaluated by the same method. Squares represent ^{230}Th-normalized $CaCO_3$ fluxes for surface-most samples from multicores (Table 1). Triangles represent average ^{230}Th-normalized $CaCO_3$ fluxes at the time of maximum flux during the last glacial period, nominally during Marine Isotope Stage 3 and approximately between 30 and 50 ka (Fig. 5). Circles with error bars reflect published evidence that there is little net accumulation of $CaCO_3$ at these sites today, based on modeling ^{230}Th profiles (Berelson et al., 1997; Stephens and Kadko, 1997) and based on the balance between $CaCO_3$ dissolution evaluated using benthic flux chambers and $CaCO_3$ rain rates collected using sediment traps (Berelson et al., 1997). The arrow at 5°N represents chemical erosion that is evident in the ^{14}C ages of MC112 (Section 5.4.1). Core-top results are available at 3°S (MC27) and at 5°N (MC112) where there are no data from corresponding piston or gravity cores. MIS3 values are available at 4°N (PC114) where there is no corresponding multicore.

Please cite this article as: Anderson, R.F., et al., Modern $CaCO_3$ preservation in equatorial Pacific sediments in the context of late-Pleistocene glacial cycles, Marine Chemistry (2007), doi:10.1016/j.marchem.2007.11.011

to El Niño conditions that existed in 1992 (Berelson et al., 1997).

Some of the $CaCO_3$ dissolution in equatorial Pacific sediments is driven by respiratory CO_2 released into pore waters. However, the organic carbon to $CaCO_3$ rain ratio in this region is low (molar ratio of ~0.6), so most $CaCO_3$ dissolution is driven by bottom water undersaturation (i.e., by the carbonate ion concentration, Berelson et al., 1997). Therefore, the large difference between modern rain rates and maximum preserved $CaCO_3$ fluxes (Fig. 12) suggests that bottom waters in this region were substantially undersaturated with respect to calcite solubility throughout the last glacial cycle.

In principle, one could estimate the change in carbonate ion concentration of bottom waters using the difference between maximum and minimum preserved $CaCO_3$ fluxes, assuming (1) no change in $CaCO_3$ production (Section 5.2) and (2) that changes in $CaCO_3$ preservation were determined exclusively by variability of the carbonate ion concentration of deep water. Unfortunately, here we encounter problems inherent in any technique used to evaluate $CaCO_3$ accumulation rates. Specifically, negative values associated with chemical erosion are undefined, and preserved $CaCO_3$ fluxes during transient periods of minimum preservation will be overestimated due to the mixing of $CaCO_3$-rich and $CaCO_3$-poor sediments by bioturbation.

The tendency to overestimate preserved $CaCO_3$ fluxes at times of minimum $CaCO_3$ preservation (e.g., today) can be illustrated by comparing ^{230}Th-normalized $CaCO_3$ fluxes for surface sediments of multicores (squares in Fig. 12) against independent estimates of $CaCO_3$ preservation or dissolution. The most extreme discrepancy between ^{230}Th-normalized $CaCO_3$ flux and the actual preserved flux occurs at 5°N (MC112), where ^{14}C ages indicate intense chemical erosion (Section 5.4.1; i.e., the actual preserved flux is negative), whereas the corresponding ^{230}Th-normalized $CaCO_3$ flux for surface sediments is 0.23 g cm^{-2} kyr^{-1}. Chemical erosion may also be occurring at 2°N and at 5°S as indicated by ^{14}C ages of surface sediments (see above) as well as by modeling of ^{230}Th profiles (Berelson et al., 1997; Stephens and Kadko, 1997). Furthermore, within the uncertainty of the fluxes measured using benthic chambers and sediment traps, there is no net accumulation of $CaCO_3$ today at the equator, 2°N or 2°S (Berelson et al., 1997). That is, the actual net accumulation of $CaCO_3$ today at these sites must be close to zero, and may be negative (circles with error bars in Fig. 12), whereas ^{230}Th-normalized $CaCO_3$ fluxes at 2°N, 0°, 2°S and 5°S are 0.33, 0.47, 0.50 and 0.42 g cm^{-2} kyr^{-1}, respectively. Therefore, the difference between maximum (MIS3; triangles) and modern (core top; squares in Fig. 12) ^{230}Th-normalized $CaCO_3$ fluxes at these sites, which amounts to 0.4 to 0.6 g cm^{-2} kyr^{-1}, must be a lower limit.

If, today, the preserved flux of $CaCO_3$ at the equator, 2°N and 2°S is close to zero (circles in Fig. 12), then this constrains the difference between maximum and minimum preserved $CaCO_3$ fluxes to be about 1 g cm^{-2} kyr^{-1}, or 0.27 mmol m^{-2} d^{-1}. Using the model of Berelson et al. (1997), this increase in $CaCO_3$ dissolution corresponds to a decrease in carbonate ion concentration of 10–12 μmol kg^{-1} (see their Fig. 15). Of course, there is substantial uncertainty in the actual difference between maximum and minimum preserved $CaCO_3$ flux, as described above, and the inferred change in carbonate ion concentration is also model dependent. Furthermore, if sediment focusing has added $CaCO_3$ to the sites studied here (Section 5.1), then the true difference between maximum and minimum $CaCO_3$ preserved flux is greater than that estimated using the ^{230}Th technique, and the decrease in carbonate ion concentration would have been greater than 10–12 μmol kg^{-1}. Nevertheless, this estimate is consistent with the 12 μmol kg^{-1} Holocene reduction in carbonate ion concentration derived by Ridgwell et al. (2003) using a model of postglacial regrowth of the terrestrial biosphere together with a Holocene increase in $CaCO_3$ deposition in shallow waters. It is also within the range of estimates based on various proxies compiled by Broecker and Clark (2007). Therefore, this comparison places useful constraints on the changes in deepwater carbonate ion concentration that were responsible for variable $CaCO_3$ preservation in equatorial Pacific sediments. Future modeling efforts that take into account the effects of sediment focusing, or that use results from sites that are unaffected by sediment focusing, will provide more reliable estimates of past changes in deepwater carbonate ion concentration.

5.5. Implications for the duration of the Holocene

The late-Holocene increase in $CaCO_3$ dissolution is relevant to the ongoing debate concerning the expected duration of the Holocene in the absence of perturbation by anthropogenic greenhouse gases (e.g., McManus et al., 2003; Augustin et al., 2004; Ruddiman, 2005; Ruddiman et al., 2005). Paleoclimatologists have long expressed concern that the warm, stable climate of the Holocene may be near its end (for an interesting historical anecdote see Broecker, 1998). More recently, this concern has grown into a debate, as scientists look to

Please cite this article as: Anderson, R.F., et al., Modern $CaCO_3$ preservation in equatorial Pacific sediments in the context of late-Pleistocene glacial cycles, Marine Chemistry (2007), doi:10.1016/j.marchem.2007.11.011

records of past climate variability for clues about earth's future.

Glacial–interglacial climate variability is regulated by summer solar insolation at high northern latitudes (Hays et al., 1976). Recent interglacials have lasted for about 10,000 years, or one half of a precession cycle (Ruddiman, 2005). The Holocene has already extended to 12,000 years, leading to the view that its end is overdue (Ruddiman et al., 2005). However, the last time that earth's orbital parameters were similar to those that occur today (i.e., low eccentricity), during MIS 11 roughly 400,000 years ago, the earth experienced an unusually long (~28,000 years) interglacial period, leading some to suggest that the Holocene may endure for another 16,000 years (Berger and Loutre, 2002; Augustin et al., 2004), and perhaps much longer (McManus et al., 2003).

Current debate centers not on the duration of MIS 11 (e.g., McManus et al., 2003), but on how best to align the present day with the MIS 11 record. Some investigators (e.g., McManus et al., 2003; Augustin et al., 2004) aligned the glacial termination preceding MIS 11 with the most recent termination, roughly between 18 and 12 ka. That alignment places today's equivalent conditions at between 405 and 410 ka and, by analogy with the MIS 11 record, the Holocene could last for another 16,000 years. Taking a different approach, Ruddiman (2005) argued that a more appropriate alignment is to link present insolation with conditions that existed at 398 ka, at a time when continental ice sheets had already started to advance. Following that analogy, Ruddiman argued that the Holocene should already have come to an end, and that northern hemisphere ice sheets should have started growing a few thousand years ago (Ruddiman, 2005; Ruddiman et al., 2005).

How are deep-sea $CaCO_3$ records relevant to this debate? As noted above, $CaCO_3$ dissolution increased dramatically prior to, and during, the initial stages of ice sheet growth for each of the late-Pleistocene glacial periods (Fig. 3). Today, the ^{230}Th-normalized flux of $CaCO_3$ in equatorial Pacific surface sediments has dropped nearly to the level that existed 100,000 years ago when ice sheets were growing (Fig. 4). Furthermore, as noted in the preceding section, bioturbation creates an inherent lag in the sediment record, such that the average conditions that are recorded in the mixed layer represent those that existed several thousand years ago, not today. Using direct measurements of $CaCO_3$ dissolution (Berelson et al., 1997), one sees that the actual preserved $CaCO_3$ flux today has dropped to a very low value, with chemical erosion at some sites and little net $CaCO_3$ accumulation at others. If these conditions were to persist for sufficiently long for the bioturbated layer to come to steady state with respect to supply and loss of $CaCO_3$, then the ^{230}Th-normalized $CaCO_3$ flux could well become as low as the minimum values of the late Pleistocene (Fig. 4) even without a further decrease in $CaCO_3$ preservation. Does this mean that the end of the Holocene is necessarily near? Comparison with records from MIS 11, and other interglacial periods, may help answer this question.

Some remarkable similarities are evident when we compare the Holocene with the $CaCO_3$ record of MIS 11. For example, the highest $CaCO_3$ contents of the PC72 record occurred during MIS 12 (roughly 440–460 ka) and during the last glacial period (30–60 ka; Fig. 3). Following these maxima, the $CaCO_3$ content dropped slowly for ~30 kyr in each case (440–410 ka and 30 ka to the core top). At about 410 ka the $CaCO_3$ content plummeted, indicating the onset of intense $CaCO_3$ dissolution (Fig. 3). The absolute age assigned to this feature is subject to some uncertainty, but the sharp drop in percent $CaCO_3$ coincides with the rise in $\delta^{18}O$ values (Fig. 3), indicating growth of continental ice sheets.

Sediment records from the central equatorial Pacific Ocean lack the temporal resolution needed to estimate accurately the duration of the interval between the increase in $CaCO_3$ dissolution and the end of the corresponding interglacial period. Therefore, we return to the benchmark record from ODP Site 1089, which has superior temporal resolution due to its high accumulation rate (roughly an order of magnitude greater than in TT013-PC72). Among the interglacial periods recorded in sediments from ODP Site 1089 there is substantial variability in the duration of the interval between the rapid decline in $CaCO_3$ content and the end of the interglacial, as marked by increasing $\delta^{18}O$ values (Fig. 13). At one extreme, during MIS 7 at ~245 ka, increasing $\delta^{18}O$ tracked declining $CaCO_3$ content with hardly any lag at all. By the time that the $CaCO_3$ content had dropped to modern (core top) values (~20%), $\delta^{18}O$ had increased from its minimum value by nearly 0.4 per mill, indicating that glaciation was well underway. At the other extreme, during MIS 11, the $CaCO_3$ content of ODP 1089 sediments had dropped to the modern value of 20% at about 413 ka, roughly 5 kyr before the minimum in global ice volume, as expressed in the $\delta^{18}O$ record (for illustration in greater detail, see Hodell et al., 2003). Altogether, ~15 kyr elapsed between the time that the $CaCO_3$ content reached its modern value (413 ka) and the point at which $\delta^{18}O$ started to increase rapidly (398 ka, Fig. 13, see also Hodell et al., 2003).

Please cite this article as: Anderson, R.F., et al., Modern $CaCO_3$ preservation in equatorial Pacific sediments in the context of late-Pleistocene glacial cycles, Marine Chemistry (2007), doi:10.1016/j.marchem.2007.11.011

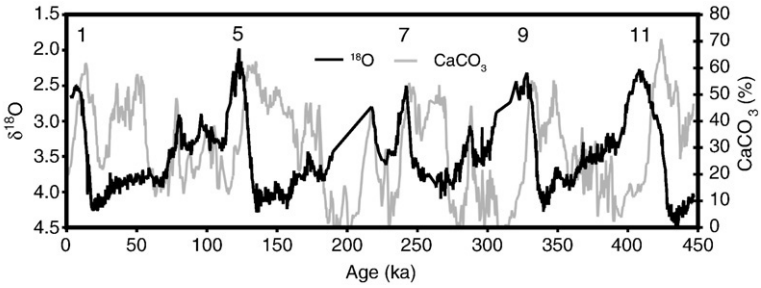

Fig. 13. Oxygen isotopic composition of benthic foraminifera (black line) and $CaCO_3$ content (grey line) of sediments from ODP Site 1089 in the Cape Basin. Peak interglacials, corresponding to minima in $\delta^{18}O$, are indicated according to the Marine Isotope Stage. Results are from Hodell et al. (2001) and are available at http://www-odp.tamu.edu/publications/177_SR/VOLUME/TABLES/SR177_09/09_T02.TXT. In intervals without oxygen isotope data the $CaCO_3$ was so dissolved that useful specimens of *C. wuellerstorfi* could not be recovered.

Therefore, although the carbonate chemistry of the deep ocean has already made the change expected to precede the transition into the next ice age, by analogy with MIS 11 this does not preclude an extended duration of the Holocene.

Hodell et al. (2003) cautioned against using MIS 11 as an analog for the Holocene because it occurred within the middle of the Mid-Brunhes carbonate dissolution cycle (see also Barker et al., 2006), indicating that the ocean's carbonate system then was different from conditions that have existed more recently. However, the principal trend over the past 500 kyr involves periods of maximum $CaCO_3$ dissolution, not periods of maximum $CaCO_3$ preservation (Fig. 7A). Calcium carbonate minima (maximum dissolution) have become less intense over the past 300 kyr, whereas there is no systematic trend in $CaCO_3$ maxima (maximum preservation). Whatever the combination of processes that has regulated late-glacial periods of maximum $CaCO_3$ preservation, these seem to have changed little throughout the late-Brunhes carbonate dissolution cycle. Therefore, whereas the intensity of $CaCO_3$ dissolution during the transition into MIS 11 may have been greater than during more recent interglacial–glacial transitions, the overall sequence of events remains unchanged. During each of the late-Pleistocene glacial cycles, changes in deep-sea carbonate chemistry, as reflected by $CaCO_3$ preservation, preceded the onset of continental glaciation. The Holocene sediment record informs us that a similar change in deep-sea carbonate chemistry has already occurred, but it does not help constrain the expected duration of the Holocene. Of course, debate about the expected duration of the Holocene may be largely academic if anthropogenic emission of greenhouse gases prevents the initiation of the next ice age for another 500,000 years, as suggested by recent models (Archer and Ganopolski, 2005).

6. Conclusions

We have presented evidence in support of the following points:

1) Two geochemical proxies for export production, ^{230}Th-normalized barite accumulation rates and ^{10}Be/^{230}Th ratios, fail to show the positive correlation expected if the patterns of $CaCO_3$ accumulation in equatorial Pacific sediments were regulated by changes in biological productivity. Similarly, Zhang et al. (2007) recently reported no correlation between $CaCO_3$ preservation and paleoproductivity proxies at sites in the western equatorial Pacific Ocean. Therefore, we conclude that glacial cycles of $CaCO_3$ accumulation are regulated by variable preservation and not by variable production.
2) Internal consistency among the records of $CaCO_3$ accumulation in sediments from the equatorial Pacific, Indian and Subantarctic Southern Oceans further supports the view that variability of $CaCO_3$ accumulation is regulated by changes in preservation that are linked to changes in deep ocean carbonate chemistry.
3) Dissolution of $CaCO_3$ in equatorial Pacific sediments has intensified during the late Holocene, having now reached an intensity that is comparable to that which occurred during the onset of each of the late-Pleistocene periods of glaciation. Extrapolating from the robust relationship that has characterized at least the past 500 kyr, we conclude that the ocean's carbonate chemistry has already made the transition that would lead into the next period of continental ice sheet growth. However, among the last four interglacial to glacial transitions, there is sufficient variability in the duration of the interval between increased $CaCO_3$ dissolution and the onset of continental ice sheet growth that the late-Holocene increase in $CaCO_3$

Please cite this article as: Anderson, R.F., et al., Modern $CaCO_3$ preservation in equatorial Pacific sediments in the context of late-Pleistocene glacial cycles, Marine Chemistry (2007), doi:10.1016/j.marchem.2007.11.011

dissolution cannot be used to infer whether the end of the Holocene is overdue, or if the current warm stable conditions would endure for several thousand years, even in the absence of human influence.

Acknowledgements

Comments on earlier versions of this manuscript by Dave Hodell, Jerry McManus, Appy Sluijs, Martin Ziegler and Mary-Elena Carr led to substantial improvements. Help from Steve Carey and the core repository staff at the University of Rhode Island, who have filled many sample requests, is much appreciated. Results presented here were generated for multiple projects, supported at various times throughout the past 15 years by the US National Science Foundation and by a grants/cooperative agreement from the National Oceanic and Atmospheric Administration. The views expressed herein are those of the authors and do not necessarily reflect the views of NOAA or any of its sub-agencies. This paper has been prepared for a special volume honoring Peter Brewer on the occasion of his 65th birthday. Three links to Peter Brewer's career can be identified in this work. First, Peter was a pioneer in the study of the ocean's carbonate chemistry, which underlies the interpretation of the results described in this paper. Second, he led the US JGOFS program at the time when the equatorial Pacific process study was planned. That study provided both the cores used here and the evidence for intense modern $CaCO_3$ dissolution that is critical to our conclusions. Finally, the senior author learned the principles and nuances of the analytical chemistry of uranium series radionuclides while working as a graduate student in Peter's lab. The senior author has enjoyed three decades interacting with Peter as a colleague and as a friend, for which he is extremely grateful.

Appendix A. Supplementary data

Supplementary data associated with this article can be found, in the online version, at doi:10.1016/j.marchem.2007.11.011.

References

Anderson, R.F., Fleisher, M.Q., Lao, Y., 2006. Glacial-interglacial variability in the delivery of dust to the central equatorial Pacific Ocean. Earth and Planetary Science Letters 242, 406–414.

Archer, D., 1991. Equatorial Pacific calcite preservation cycles: production or dissolution? Paleoceanography 6 (5), 561–571.

Archer, D., Ganopolski, A., 2005. A movable trigger: fossil fuel CO_2 and the onset of the next glaciation. Geochemistry Geophysics Geosystems 6, Q05003. doi:10.1029/2004GC000891.

Arrhenius, G., 1952. Sediment cores from the east Pacific. In: Pettersson, H. (Ed.), Reports of the Swedish deep sea expedition, 1947–1948, p. 201.

Arrhenius, G., 1988. Rate of production, dissolution and accumulation of biogenic solids in the ocean. Palaeogeography Palaeoclimatology Palaeoecology 67 (1–2), 119–146.

Augustin, L., Barbante, C., Barnes, P.R.F., Barnola, J.M., Bigler, M., Castellano, E., Cattani, O., Chappellaz, J., Dahl-Jensen, D., Delmonte, B., Dreyfus, G., Durand, G., Falourd, S., Fischer, H., Fluckiger, J., Hansson, M.E., Huybrechts, P., Jugie, R., Johnsen, S.J., Jouzel, J., Kaufmann, P., Kipfstuhl, J., Lambert, F., Lipenkov, V.Y., Littot, G.V.C., Longinelli, A., Lorrain, R., Maggi, V., Masson-Delmotte, V., Miller, H., Mulvaney, R., Oerlemans, J., Oerter, H., Orombelli, G., Parrenin, F., Peel, D.A., Petit, J.R., Raynaud, D., Ritz, C., Ruth, U., Schwander, J., Siegenthaler, U., Souchez, R., Stauffer, B., Steffensen, J.P., Stenni, B., Stocker, T.F., Tabacco, I.E., Udisti, R., van de Wal, R.S.W., van den Broeke, M., Weiss, J., Wilhelms, F., Winther, J.G., Wolff, E.W., Zucchelli, M., 2004. Eight glacial cycles from an Antarctic ice core. Nature 429 (6992), 623–628.

Bacon, M.P., 1984. Glacial to interglacial changes in carbonate and clay sedimentation in the Atlantic Ocean estimated from ^{230}Th measurements. Isotope Geoscience 2 (2), 97–111.

Barker, S., Archer, D., Booth, L., Elderfield, H., Henderiks, J., Rickaby, R.E.M., 2006. Globally increased pelagic carbonate production during Mid-Brunhes dissolution interval and the CO_2 paradox of the MIS 1. Quaternary Science Reviews 25 (23–24), 3278–3293.

Bassinot, F.C., Beaufort, L., Vincent, E., Labeyrie, L.D., Rostek, F., Muller, P.J., Quidelleur, X., Lancelot, Y., 1994. Coarse fraction fluctuations in pelagic carbonate sediments from the tropical Indian-Ocean – a 1500-Kyr record of carbonate dissolution. Paleoceanography 9 (4), 579–600.

Berelson, W.M., Anderson, R.F., Dymond, J., Demaster, D., Hammond, D.E., Collier, R., Honjo, S., Leinen, M., McManus, J., Pope, R., Smith, C., Stephens, M., 1997. Biogenic budgets of particle rain, benthic remineralization and sediment accumulation in the equatorial Pacific. Deep-Sea Research Part II-Topical Studies in Oceanography 44 (9–10), 2251–2282.

Berger, A., Loutre, M.F., 2002. An exceptionally long interglacial ahead? Science 297, 1287–1288.

Berger, W.H., 1992. Pacific carbonate cycles revisited: arguments for and against productivity control. In: Ishizaki, K., Saito, T. (Eds.), Centenary of Japanese Micropaleontology. Terra Scientific Publishing Company, Tokyo, pp. 15–25.

Bishop, J.K.B., 1988. The barite-opal-organic carbon association in oceanic particulate matter. Nature 332 (6162), 341–343.

Bradtmiller, L.I., Anderson, R.F., Fleisher, M.Q., Burckle, L.H., 2006. Diatom productivity in the equatorial Pacific Ocean from the last glacial period to the present: a test of the silicic acid leakage hypothesis. Paleoceanography 21, PA4201. doi:10.1029/2006PA001282.

Broecker, W.S., 1998. The end of the present interglacial: how and when? Quaternary Science Reviews 17 (8), 689–694.

Broecker, W., Clark, E., 2007. Is the magnitude of the carbonate ion decrease in the abyssal ocean over the last 8 kyrs consistent with the 20 ppm rise in atmospheric CO_2 content? Paleoceanography 22, PA1202. doi:10.1029/2006PA001311.

Broecker, W.S., Klas, M., Clark, E., Bonani, G., Ivy, S., Wolfli, W., 1991. The influence of $CaCO_3$ dissolution on core top radiocarbon ages for deep-sea sediments. Paleoceanography 6 (5), 593–608.

Chase, Z., Anderson, R.F., Fleisher, M.Q., Kubik, P., 2002. The influence of particle composition on scavenging of Th, Pa and Be in the ocean. Earth and Planetary Science Letters 204, 215–229.

Chase, Z., Anderson, R.F., Fleisher, M.Q., Kubik, P., 2003. Accumulation of biogenic and lithogenic material in the Pacific sector of the Southern Ocean during the past 40,000 years. Deep-Sea Research II 50, 799–832.

Dehairs, F., Chesselet, R., Jedwab, J., 1980. Discrete suspended particles of barite and the barium cycle in the open ocean. Earth and Planetary Science Letters 49 (2), 528–550.

Dehairs, F., Baeyens, W., Goeyens, L., 1992. Accumulation of suspended barite at mesopelagic depths and export production in the Southern Ocean. Science 258 (5086), 1332–1335.

Dymond, J., Suess, E., Lyle, M., 1992. Barium in deep-sea sediment: a geochemical proxy for paleoproductivity. Paleoceanography 7 (2), 163–181.

Fagel, N., Andre, L., Dehairs, F., 1999. Advective excess Ba transport as shown from sediment and trap geochemical signatures. Geochimica et Cosmochimica Acta 63 (16), 2353–2367.

Fagel, N., Dehairs, F., Peinert, R., Antia, A., Andre, L., 2004. Reconstructing export production at the NE Atlantic margin: potential and limits of the Ba proxy. Marine Geology 204, 11–25.

Fairbanks, R.G., Mortlock, R.A., Chiu, T.C., Cao, L., Kaplan, A., Guilderson, T.P., Fairbanks, T.W., Bloom, A.L., Grootes, P.M., Nadeau, M.J., 2005. Radiocarbon calibration curve spanning 0 to 50,000 years BP based on paired $^{230}Th/^{234}U/^{238}U$ and ^{14}C dates on pristine corals. Quaternary Science Reviews 24 (16–17), 1781–1796.

Farrell, J.W., Prell, W.L., 1989. Climatic change and $CaCO_3$ preservation: An 800,000 year bathymetric reconstruction from the central equatorial Pacific Ocean. Paleoceanography 4 (4), 447–466.

Francois, R., Bacon, M., Suman, D.O., 1990. Thorium 230 profiling in deep-sea sediments: High-resolution records of flux and dissolution of carbonate in the equatorial Atlantic during the last 24,000 years. Paleoceanography 5 (5), 761–787.

Francois, R., Honjo, S., Manganini, S.J., Ravizza, G.E., 1995. Biogenic barium fluxes to the deep-sea – implications for paleoproductivity reconstruction. Global Biogeochemical Cycles 9 (2), 289–303.

Francois, R., Frank, M., Rutgers van der Loeff, M.M., Bacon, M.P., 2004. Th-230 normalization: an essential tool for interpreting sedimentary fluxes during the late Quaternary. Paleoceanography 19 (1), PA1018. doi:10.1029/2003PA000939.

Francois, R., Frank, M., van der Loeff, M.R., Bacon, M.P., Geibert, W., Kienast, S., Anderson, R.F., Bradtmiller, L., Chase, Z., Henderson, G., Marcantonio, F., Allen, S.E., 2007. Comment on "Do geochemical estimates of sediment focusing pass the sediment test in the equatorial Pacific?" by M. Lyle et al. Paleoceanography 22 (1), PA1216. doi:10.1029/2005PA001235.

Hays, J.D., Imbrie, J., Shackleton, N.J., 1976. Variations in earths orbit – pacemaker of ice ages. Science 194 (4270), 1121–1132.

Henderson, G.M., Heinze, C., Anderson, R.F., Winguth, A.M.E., 1999. Global distribution of the ^{230}Th flux to ocean sediments constrained by GCM modelling. Deep-Sea Research Part I-Oceanographic Research Papers 46 (11), 1861–1893.

Hodell, D.A., Charles, C.D., Sierro, F.J., 2001. Late Pleistocene evolution of the ocean's carbonate system. Earth and Planetary Science Letters 192 (2), 109–124.

Hodell, D.A., Kanfoush, S.L., Venz, K.A., Charles, C.D., Sierro, F.J., 2003. The Mid-Brunhes transition in ODP Sites 1089 and 1090 (Subantarctic South Atlantic). In: Droxler, A.W., Poore, R.Z., Burkle, L.H. (Eds.), Earth's Climate and Orbital Eccentricity: The Marine Isotope Stage 11 Question. American Geophysical Union, Washington, pp. 113–129.

Honjo, S., Dymond, J., Collier, R., Manganini, S.J., 1995. Export production of particles to the interior of the Equatorial Pacific-Ocean during the 1992 EqPac experiment. Deep-Sea Research Part II-Topical Studies in Oceanography 42 (2–3), 831–870.

Keir, R.S., Berger, W.H., 1985. Late Holocene carbonate dissolution in the equatorial Pacific: reef growth or neoglaciation? In: Sundquist, E.T., Broecker, W.S. (Eds.), The Carbon Cycle and Atmospheric CO_2: Natural Variations Archean to Present. Geophysical Monograph 32. American Geophysical Union, Washington D.C., pp. 208–219.

Keir, R.S., Michel, R.L., 1993. Interface dissolution control of the ^{14}C profile in marine sediment. Geochimica et Cosmochimica Acta 57 (15), 3563–3573.

Kumar, N., Anderson, R.F., Mortlock, R.A., Froelich, P.N., Kubik, P., Dittrich-Hannen, B., Suter, M., 1995. Increased biological productivity and export production in the glacial Southern Ocean. Nature 378 (6558), 675–680.

LaMontagne, R.W., Murray, R.W., Wei, K.Y., Leinen, M., Wang, C.H., 1996. Decoupling of carbonate preservation, carbonate concentration, and biogenic accumulation: A 400-kyr record from the central equatorial Pacific Ocean. Paleoceanography 11 (5), 553–562.

Lao, Y., Anderson, R.F., Broecker, W.S., Hofmann, H.J., Wolfli, W., 1993. Particulate fluxes of ^{230}Th, ^{231}Pa and ^{10}Be in the northeastern Pacific Ocean. Geochimica et Cosmochimica Acta 57, 205–217.

Le, J., Shackleton, N.J., 1992. Carbonate dissolution fluctuations in the western equatorial Pacific during the late Quaternary. Paleoceanography 7 (1), 21–42.

Lisiecki, L.E., Raymo, M.E., 2005. A Pliocene–Pleistocene stack of 57 globally distributed benthic $\delta^{18}O$ records. Paleoceanography 20 (1), PA1003. doi:10.1029/2004PA001071.

Lochte, K., Anderson, R.F., Francois, R., Jahnke, R.A., Shimmield, G., Vetrov, A., 2003. Benthic processes and the burial of carbon. In: Fasham, M.J.R. (Ed.), Ocean Biogeochemistry: The Role of the Ocean Carbon Cycle in Global Change. Springer-Verlag, Berlin, pp. 196–216.

Loubere, P., Richaud, M., 2007. Some reconciliation of glacial–interglacial calcite flux reconstructions for the eastern equatorial Pacific. Geochemistry Geophysics Geosystems 8, Q03008. doi:10.1029/2006GC001367.

Loubere, P., Mekik, F., Francois, R., Pichat, S., 2004. Export fluxes of calcite in the eastern equatorial Pacific from the last glacial maximum to present. Paleoceanography 19 (2), PA2018. doi:10.1029/2003PA000986.

Lyle, M., Murray, D.W., Finney, B.P., Dymond, J., Robbins, J.M., Brooksforce, K., 1988. The record of late Pleistocene biogenic sedimentation in the eastern tropical Pacific Ocean. Paleoceanography 3, 39–59.

Lyle, M., Mitchell, N., Pisias, N., Mix, A., Martinez, J.I., Paytan, A., 2005. Do geochemical estimates of sediment focusing pass the sediment test in the equatorial Pacific? Paleoceanography 20, PA1005. doi:10.1029/2004PA001019.

Lyle, M., Pisias, N., Paytan, A., Martinez, J.I., Mix, A., 2007. Reply to comment by R. Francois et al. on "Do geochemical estimates of sediment focusing pass the sediment test in the equatorial Pacific?": further explorations of Th-230 normalization. Paleoceanography 22 (1), PA1217. doi:10.1029/2006PA001373.

Marcantonio, F., Anderson, R.F., Stute, M., Kumar, N., Schlosser, P., Mix, A., 1996. Extraterrestrial ^{3}He as a tracer of marine sediment transport and accumulation. Nature 383 (6602), 705–707.

Please cite this article as: Anderson, R.F., et al., Modern $CaCO_3$ preservation in equatorial Pacific sediments in the context of late-Pleistocene glacial cycles, Marine Chemistry (2007), doi:10.1016/j.marchem.2007.11.011

Marcantonio, F., Anderson, R.F., Higgins, S., Stute, M., Schlosser, P., Kubik, P., 2001. Sediment focusing in the central equatorial Pacific Ocean. Paleoceanography 16 (3), 260–267.

McManus, J., Berelson, W.M., Klinkhammer, G.P., Johnson, K.S., Coale, K.H., Anderson, R.F., Kumar, N., Burdige, D.J., Hammond, D.E., Brumsack, H.J., McCorkle, D.C., Rushdi, A., 1998. Geochemistry of barium in marine sediments: implications for its use as a paleoproxy. Geochimica et Cosmochimica Acta 62 (21–22), 3453–3473.

McManus, J., Oppo, D., Cullen, J., Healey, S., 2003. Marine isotope stage 11 (MIS 11): analog for Holocene and future climate? In: Droxler, A.W., Poore, R.Z., Burkle, L.H. (Eds.), Earth's climate and orbital eccentricity: the marine isotope stage 11 question. American Geophysical Union, Washington, pp. 69–85.

Mekik, F.A., Loubere, P.W., Archer, D.E., 2002. Organic carbon flux and organic carbon to calcite flux ratio recorded in deep-sea carbonates: demonstration and a new proxy. Global Biogeochemical Cycles 16. doi:10.1029/2001GB001634.

Murray, R.W., Leinen, M., 1993. Chemical-transport to the seafloor of the equatorial Pacific Ocean across a latitudinal transect at 135°W – tracking sedimentary major, trace, and rare-earth element fluxes at the equator and the intertropical convergence zone. Geochimica et Cosmochimica Acta 57 (17), 4141–4163.

Murray, R.W., Leinen, M., Murray, D.W., Mix, A.C., Knowlton, C.W., 1995. Terrigenous Fe Input and biogenic sedimentation in the glacial and interglacial equatorial Pacific-Ocean. Global Biogeochemical Cycles 9 (4), 667–684.

Murray, R.W., Knowlton, C., Leinen, M., Mix, A.C., Polsky, C.H., 2000. Export production and carbonate dissolution in the central equatorial Pacific Ocean over the past 1 Myr. Paleoceanography 15 (6), 570–592.

Paytan, A., 1995. Marine barite, a recorder of ocean chemistry, productivity, and circulation. Ph.D. Thesis, University of California, San Diego, San Diego, CA, 111 pp.

Pedersen, T.F., 1983. Increased productivity in the eastern equatorial Pacific during the last glacial maximum (19,000 to 14,000 Yr BP). Geology 11 (1), 16–19.

Peterson, L.C., Prell, W.L., 1985. Carbonate preservation and rates of climatic change: an 800 kyr record from the Indian Ocean. In: Sundquist, E.T., Broecker, W.S. (Eds.), The Carbon Cycle and Atmospheric CO_2: Natural Variations Archaen to Present. Geophysical Monograph 32. American Geophysical Union, Washington, D. C., pp. 251–270.

Reimer, P.J., Baillie, M.G.L., Bard, E., Bayliss, A., Beck, J.W., Bertrand, C.J.H., Blackwell, P.G., Buck, C.E., Burr, G.S., Cutler, K.B., Damon, P.E., Edwards, R.L., Fairbanks, R.G., Friedrich, M., Guilderson, T.P., Hogg, A.G., Hughen, K.A., Kromer, B., McCormac, G., Manning, S., Ramsey, C.B., Reimer, R.W., Remmele, S., Southon, J.R., Stuiver, M., Talamo, S., Taylor, F.W., van der Plicht, J., Weyhenmeyer, C.E., 2004. IntCal04 terrestrial radiocarbon age calibration, 0–26 cal kyr BP. Radiocarbon 46 (3), 1029–1058.

Ridgwell, A.J., Watson, A.J., Maslin, M.A., Kaplan, J.O., 2003. Implications of coral reef buildup for the controls on atmospheric CO_2 since the last glacial maximum. Paleoceanography 18 (4), 1083. doi:10.1029/2003PA000893.

Ruddiman, W.F., 2005. Cold climate during the closest Stage 11 analog to recent millennia. Quaternary Science Reviews 24 (10–11), 1111–1121.

Ruddiman, W.F., Vavrus, S.J., Kutzbach, J.E., 2005. A test of the overdue-glaciation hypothesis. Quaternary Science Reviews 24 (1–2), 1–10.

Scholten, J.C., Fietzke, J., Vogler, S., Rutgers van der Loeff, M.M., Mangini, A., Koeve, W., Waniek, J., Stoffers, P., Antia, A., Kuss, J., 2001. Trapping efficiencies of sediment traps from the deep eastern North Atlantic: the ^{230}Th calibration. Deep-Sea Research II 48, 2383–2408.

Scholten, J.C., Fietzke, J., Mangini, A., Stoffers, P., Rixen, T., Gaye-Haake, B., Blanz, T., Ramaswamy, V., Sirocko, F., Schulz, H., Ittekkot, V., 2004. Radionuclide fluxes in the Arabian Sea: the role of particle composition. Earth and Planetary Science Letters 230, 319–337.

Siddall, M., Henderson, G.M., Edwards, N.R., Frank, M., Mueller, S.A., Stocker, T.F., Joos, F., 2005. ^{231}Pa/^{230}Th fractionation by ocean transport, biogenic particle flux and particle type. Earth and Planetary Science Letters 237, 135–155.

Stephens, M.P., Kadko, D.C., 1997. Glacial-Holocene calcium carbonate dissolution at the central equatorial Pacific seafloor. Paleoceanography 12 (6), 797–804.

Stuiver, M., Reimer, P.J., 1993. Extended ^{14}C data-base and revised Calib 3.0 ^{14}C age calibration program. Radiocarbon 35 (1), 215–230.

Thomas, E., Turekian, K.K., Wei, K.Y., 2000. Productivity control of fine particle transport to equatorial Pacific sediment. Global Biogeochemical Cycles 14 (3), 945–955.

Winckler, G., Anderson, R.F., Schlosser, P., 2005. Equatorial Pacific productivity and dust flux during the mid-Pleistocene climate transition. Paleoceanography 20, PA4025. doi:10.1029/2005PA001177.

Yang, Y.L., Elderfield, H., Ivanovich, M., 1990. Glacial to Holocene changes in carbonate and clay sedimentation in the equatorial Pacific Ocean estimated from Thorium 230 profiles. Paleoceanography 5 (5), 789–809.

Yu, E.F., Francois, R., Bacon, M.P., Fleer, A.P., 2001a. Fluxes of ^{230}Th and ^{231}Pa to the deep sea: Implications for the interpretation of excess ^{230}Th and ^{231}Pa/^{230}Th profiles in sediments. Earth and Planetary Science Letters 191, 219–230.

Yu, E.F., Francois, R., Bacon, M.P., Honjo, S., Fleer, A.P., Manganini, S.J., van der Loeff, M.M.R., Ittekot, V., 2001b. Trapping efficiency of bottom-tethered sediment traps estimated from the intercepted fluxes of ^{230}Th and ^{231}Pa. Deep-Sea Research Part I-Oceanographic Research Papers 48 (3), 865–889.

Zhang, J., Wang, P., Li, Q., Cheng, X., Jin, H., Zhang, S., 2007. Western equatorial Pacific productivity and carbonate dissolution over the last 550 kyr: foraminiferal and nannofossil evidence from ODP Hole 807A. Marine Micropaleontology 64, 121–140.

Please cite this article as: Anderson, R.F., et al., Modern $CaCO_3$ preservation in equatorial Pacific sediments in the context of late-Pleistocene glacial cycles, Marine Chemistry (2007), doi:10.1016/j.marchem.2007.11.011